ELSEVIER

Analytica Chimica Acta 431 (2001) 169–180

ANALYTICA CHIMICA ACTA

www.elsevier.com/locate/aca

Measurement of nitrogen dioxide and nitrous acid using gas-permeable liquid core waveguides

Marcio R. Milani[1], Purnendu K. Dasgupta*

Department of Chemistry, Texas Tech University, Lubbock, TX 79409-1061, USA

Received 3 August 2000; accepted 21 November 2000

Abstract

Nitrogen dioxide is an important atmospheric contaminant, classified as a criteria pollutant in the United States. It can be sensitively determined by the simple colorimetric Griess–Saltzmann method. This can constitute the basis of an inexpensive sensitive instrument based on gas-permeable liquid core waveguide tubes that allow long path absorbance measurement. Nitrous (HONO) acid is often present in the atmosphere along with NO_2. Nitrous acid concentration can be significant relative to NO_2, especially at night-time when photodecomposition of HONO is no longer operative. Griess–Saltzman chemistry cannot differentiate between HONO and NO_2. In the present paper, we have explored the possibility of simultaneously determining both analytes by using more than one collector with dimensional differences. Presented results show that differences in either length or wall thickness can permit such differentiation.

Keywords: Nitrogen dioxide; Photodecomposition; Nitrous acid

1. Introduction

Nitrogen dioxide (NO_2) and nitrous acid (HONO) play very important roles in atmospheric chemistry of nitrogen compounds. Cobb and Braman have provided a detailed review of the relationship between HONO and nitrogen oxides in the atmosphere [1]; however, the levels of day-time nitrous acid reported by these authors may be too high. Lammel and Cape have reviewed the occurrence and chemistry of atmospheric HONO and nitrites [2]. Harrison et al. have provided an thoughtful discussion of the tropospheric cycling of HONO [3]. The concentration of nitrite in orographic clouds has been taken as an indicator of HONO in rural air [4]. It has long been known that HONO is photolyzed by light ($\lambda < 390$ nm) and is thus a major source of the hydroxyl radical ($^{\bullet}$OH). Because of this destruction by sunlight, HONO levels exhibit strong diurnal variations [5]. Apparently for kinetic rather than thermodynamic reasons, automobile exhaust contains significant concentrations of HONO [6], so HONO concentrations can be very high inside automobiles [7]. HONO is also produced from atmospheric reactions of NO_2 [8,9]. Although hydrolysis of NO_2 is slow [10], it may be catalyzed by surfaces; enhanced formation of HONO during foggy periods has been observed [11]. Current research indicates that atmospheric production of HONO from NO_2 may be mediated by carbonaceous particles [12–14]. There is considerable concern about the health risks for both NO_2 and HONO [15,16]. Personal exposure to HONO

* Corresponding author. Tel.: +1-806-742-3067; fax: +1-806-742-1289.
E-mail address: sandy.dasgupta@ttu.edu (P.K. Dasgupta).
[1] Present address: Departamento de Quimica Analitica, Instituto de Quimica de Araraquara, Universidade Estadual Paulista, R. Prof. Francisco Degni S/n. C.P. 355-CEP. 14.800-900 Araraquara, SP, Brazil.

0003-2670/01/$ – see front matter
PII: S0003-2670(00)01331-3

is considerably higher indoors rather than outdoors [17–19]; open flame sources produce HONO in a significant manner [20].

In principle, it should be possible to measure both HONO and NO_2 by direct absorption spectrometery. Although HONO has commonly been measured by long path differential optical absorption spectrometry (DOAS) [5,21–25], NO_2 is rarely measured this way. Routine utility of DOAS is deterred by the relatively high instrument cost. Rodgers and Davis [26] pointed out other limitations of DOAS and proposed a photofragmentation, laser-induced fluorescence technique. Unfortunately, this technique is also very capital intensive. In the United States, NO_2 is one of the criteria air pollutants. Gas phase chemiluminescence (CL) by a difference technique is the most often used among the officially approved methods. Nevertheless, the gas phase CL-based instruments are unable to distinguish between NO_2 and HONO and have other interferences as well. There is a keen interest on the part of regulatory agencies to have an affordable instrument that will not be subject to such errors [27]. In suburban air, NO_2 and HONO levels are generally well correlated but in rural air the HONO/NO_2 ratio tends to be higher when the NO_2 concentration is more than 10 ppbv [3].

Alkaline sorbent-coated denuders provide an affordable means to measure HONO (but generally, it is not so attractive to measure NO_2 in this way because of the difficulty in achieving quantitative collection), a technique pioneered by Ferm and Sjodin [28] and followed by many others [29–34]. Good agreement between DOAS and denuder measurements has been reported [33,34]. Alkaline sorbent-coated denuders are, however, subject to artifact production of nitrite mediated by the alkaline denuder surface [32,35] or from negative errors due to the O_3-induced oxidation of the nitrite [36,37]. Several wet denuder/diffusion scrubber approaches, coupled to ion chromatography, have been developed. These provide measurements for both HNO_3 and HONO that are much less subject to error [38–41]. The results obtained with these methods indicated a small but persistent level of daytime HONO. Initially many believed that these were measurement artifacts [2], but other recent considerations indicate that such levels should actually be expected [3].

In the context of sensitive and affordable techniques, the classical Griess–Saltzman (GS) method [42] has been and is still widely used for the measurement of NO_2 [43]. The reagent cocktail contains sulfanilic acid and *N*-(1-naphthyl)ethylenediamine in a medium acidified with acetic acid. NO_2 is reduced to HONO upon hydrogen abstraction from a donor molecule in the reagent and the HONO then diazotizes sulfanilic acid. This is followed by subsequent coupling with *N*-(1-naphthyl)ethylenediamine dihydrochloride to form an azo dye. Obviously, if the method relies on the formation of HONO, it cannot distinguish NO_2 from HONO.

In recent years, liquid phase optical absorption based methods have received a most welcome boost with the commercial availability of Teflon® AF, a transparent fluoropolymer that has a refractive index less than that of water throughout the UV–VIS range. Tubes of this material can be used as liquid core waveguides (LCWs) that carry light with very little loss to the wall and as a result, long path absorption spectroscopy in the liquid phase has become practical [44–46]. Since Teflon® AF tubing is highly permeable to many gases, one approach is to use the Teflon AF tube both as the gas permeable cell and the long path absorption cell. It has been shown that such very simple devices respond to NO_2 with sufficient sensitivity for ambient air measurements [47].

The overall response of a gas permeable LCW is dependent not only on the chemistry, but also on the rate of permeation of the analyte gas through the tube. The permeation rate is thus dependent on factors that include the following: (a) the solubility of the gas in the polymer, (b) the diffusion coefficient of the analyte through the polymer, and (c) the rate at which the analyte is consumed by the interior solution. Even though NO_2 and HONO both respond to GS chemistry, these two analytes are not likely to behave in an identical fashion regarding the above properties. Can one discriminate between these gases based on the use of more than one gas permeable LCW device with, say, differing length or wall thickness, which will modulate the mass transfer differently? A gas permeable LCW coupled to a light emitting diode based absorbance detector can be constructed so inexpensively that several can be operated for the cost of one gas phase CL detector.

The object of this paper is thus to investigate if HONO and NO_2 can be simultaneously measured by using two gas permeable LCW devices and to delineate the limits of such an approach.

2. Experimental

2.1. Materials

Annular tubular devices of Teflon AF with optical fibers communicating to an AF tube through which liquid can flow and around which gas can be sampled were constructed essentially in the same fashion as described previously [47]; only a brief description follows. Two concentric tubes form the annular device: a Teflon AF 2400 capillary inside and a glass tube outside. Absorbent solution flows inside the AF capillary through a set of tees; the gas sample flows through another set of tees in the annular space. Technical grade acrylic optical fibers (0.75 mm diameter, Edmund Scientific, Barrington, NJ) that could be inserted into the particular AF capillary were used; one to bring the source light to the device and the other to carry the transmitted light to the detector. Devices were built with Teflon AF 2400 capillaries (o.d. 1.092 mm; i.d. 0.848 mm, Biogeneral Inc., San Diego, CA) with different active lengths (77, 100, 150, 227 and 277 mm, device type A). One 180 mm active length device, with an o.d. of 1.092 mm and an i.d. of 0.787 mm was also built (device B).

2.1.1. Electronics

A super luminescent green LED (Nichia 590S, 495 nm center wavelength, driven at 20 mA, www.nichia.com) was used as the light source. The LED was equipped with a photodiode (BPW 34, Siemens AG) cemented to its bottom and a similar photodiode was affixed to the free terminus of the exit fiber from the AF device. The photocurrent outputs were directly fed to a log ratio amplifier to generate the absorbance output [48] and the data were acquired with a Keithley–Metrabyte DAS 1601 12-bit data acquisition card and processed by software written in-house.

2.1.2. Gas sources

Nitrogen dioxide was generated from a permeation tube source maintained at 30°C. HONO was generated from a solid NH_4NO_2-based source [49] with a very low flow of dry N_2 (5–25 ml min^{-1}) through the source maintained at 0°C. The ammonia in the output was removed with a perfluorosulfonate Nafion® resin in the hydrogen form.

2.1.3. Generation of mixtures of NO_2 and HONO

The primary flow through the NO_2 permeation tube chamber was held constant at 250 ml min^{-1} metered by mass flow controller F_1. The exit flow was directed through a tee. The main downstream exit flow was put through a narrow bore PTFE tube representing a restriction while the vent flow through the tee arm was controlled by a needle valve N1 and measured by mass flow meter F_2. The HONO source flow ($F_3 \sim 5$ ml min^{-1}) and the net NO_2 flow ($F_1 - F_2$) were introduced into a mixing bottle containing a vent port and a further dilution flow F_4 and two sampling ports (see Fig. 1).

With a permeation rate of R (ng min^{-1}) for the NO_2 source, the final NO_2 concentration is given by $(F_1-F_2)R/(F_1(F_1-F_2+F_3+F_4))$ ng ml^{-1} (the flows F_i are given in ml min^{-1}). The NO_2 concentration was changed by changing F_2. With an HONO equilibrium concentration of C (ppbv) at the source, final HONO concentration is given by CF_3 ($F_1 - F_2 + F_3 + F_4$). The HONO concentration is changed primarily by changing F_3.

2.1.4. Reagent

The GS reagent was made according to the standard formulation [43].

2.2. Methods

2.2.1. Collection efficiency

The collection efficiency of any given device (e.g. a bubbler or an AF tube-based collector) for a given gas can be measured by using two collectors in series. As long as we operate in the domain where the blank corrected absorbance in a given device is linearly proportional to the analyte collected, the collection efficiencies each of the two devices is easily computed [50]. Let us imagine a bubbler and a second collection device are connected in series and a fixed concentration of the analyte gas passes through the system at a fixed flow rate with the bubbler being the upstream collector. After a fixed period of time, the bubbler contents are spectrophotometrically measured with the blank corrected absorbance being m_1. The upstream/downstream position of the bubbler and the other collector are now reversed, the experiment repeated and the bubbler contents now yield an absorbance of m_2. The collection efficiency (f) of the

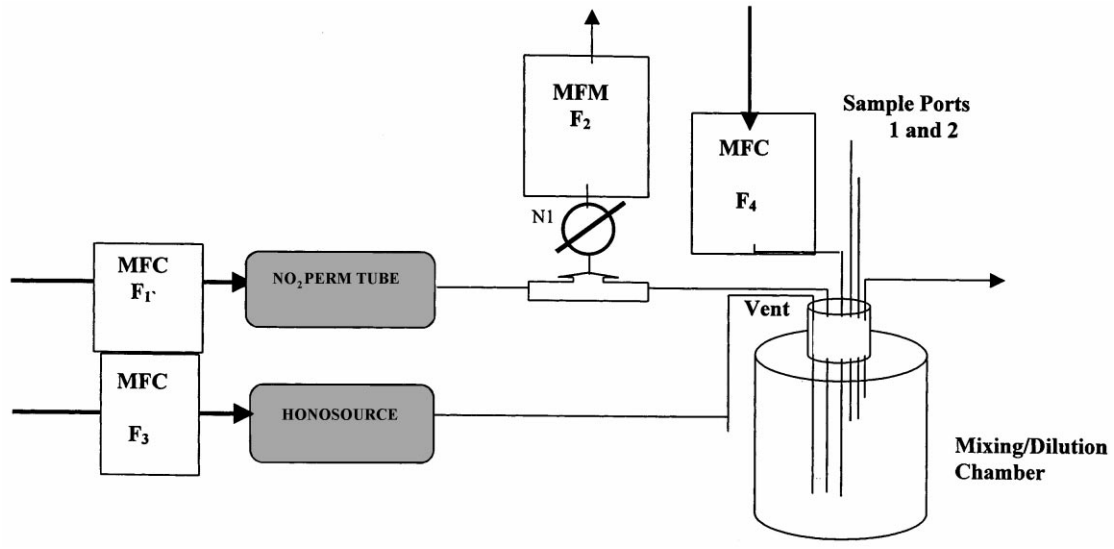

Fig. 1. Generation system for NO_2, HONO and their mixtures.

other collector will be given by [50]:

$$f = 1 - \left(\frac{m_2}{m_1}\right) \quad (1)$$

The bubbler collection efficiency for NO_2 was measured in triplicate experiments using two bubblers connected in series, each containing 10 ml of Griess–Saltzman solution. A flow of 250 ml min^{-1} was used for 60 min with a NO_2 concentration of 248 $\mu g/m^3$. Spectrophotometric measurements were carried out by a Hewlett-Packard 8451A spectrometer at 550 nm. The same procedure was employed to determine the bubbler collection efficiency for HONO. The nitrogen flow through the source was 6 ml min^{-1}; to this 250 ml min^{-1} dilution flow was merged, resulting in a HONO concentration of 240 $\mu g\, m^{-3}$. The sampling period was 60–210 min with a sampling rate of 115 ml min^{-1}.

2.2.2. Sampling of NO_2, HONO and their mixtures

Nitrous acid, NO_2 and mixtures thereof were sampled in parallel by AF device B and a bubbler through parallel streams with the sample flow rate held constant at 115 and 125 ml min^{-1}, for each stream, respectively. As previously described [47], the GS absorbing solution was held inside the AF device in a stopped flow mode for the sampling duration (60 min). The slope represented by the rate of increase of the absorbance with time is considered the response of the AF device whereas the post-sampling absorbance of the bubbler solution (10 ml) is taken to be the response of the bubbler. The presented results represent the average of multiple measurements.

AF device type A of different lengths were used to sample NO_2, HONO and NO_2 and HONO mixtures.

3. Results and discussion

3.1. Collection efficiency

The ability of a bubbler to collect HONO, an easily water soluble analyte, was presumed to be very good and the experimentally determined collection efficiency (0.9587 ± 0.0011) borne out this expectation. In contrast, the collection of NO_2 (0.5637 ± 0.0353) by a bubbler was far from quantitative. The collection efficiencies of the AF devices were both length- and flow rate-dependent, increasing with decreasing flow rate and increasing length.

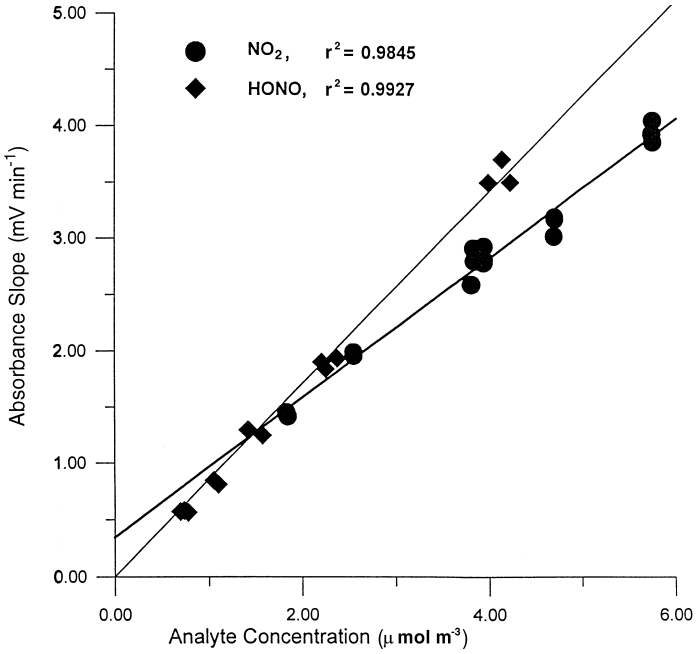

Fig. 2. Calibration plot for type B AF device for HONO and NO_2.

3.2. AF device response

In the stopped flow configuration and with exposure to a constant concentration of the analyte, the AF device produces a linear change in absorbance with time and the slope of the curve is proportional to the analyte concentration [47]. For the present 60 min experiments, the experimental slope was calculated from the data spanning the 20–40 min period. The relation between the slopes obtained at different NO_2 and HONO levels taken individually) and the test analyte concentration is shown in Fig. 2 for device B. In both cases, the observed slope is highly correlated to the test concentration. The individual calibration plots exhibit different slopes and intercepts. In the case of HONO, the behavior is normal in that the intercept is actually statistically indistinguishable from zero ($r^2 = 0.9927$). In the case of NO_2, the best fit line as shown has a small but finite intercept ($r^2 = 0.9845$). This indicates that the mechanism by which this analyte produces the analytical signal is more complex. In general, the conversion efficiency of NO_2 to nitrite (the active species leading to the chromogen) is taken in standard methods to be 0.72 [43], although it has been reported that this may be dependent on the NO_2 concentration [51]. The scatter in the data precludes a more elaborate discussion.

A set of eight experiments was then conducted with pure NO_2 and HONO and mixtures thereof ranging from [HONO] $= 0.67\,\mu\text{mol}\,\text{m}^{-3}$ and [NO_2] $= 0$ to [HONO] $= 0$ and [NO_2] $= 2.68\,\mu\text{mol}\,\text{m}^{-3}$. The experimental slopes ($\text{mV}\,\text{min}^{-1}$) observed in these experiments obeyed the relationship below with a good correlation coefficient:

$$\text{Slope} = 0.978\,[\text{NO}_2] + 1.40\,[\text{HONO}],\ r^2 = 0.9938 \quad (2)$$

The agreement between the observed slopes and those predicted from Eq. (2) are shown in Figs. 3 and 4.

In terms of isolating the contributions of HONO and NO_2 to the overall observed result, more is needed, however. Another dimension in the measurement device, length or wall thickness, must be brought in to perform such a differentiation.

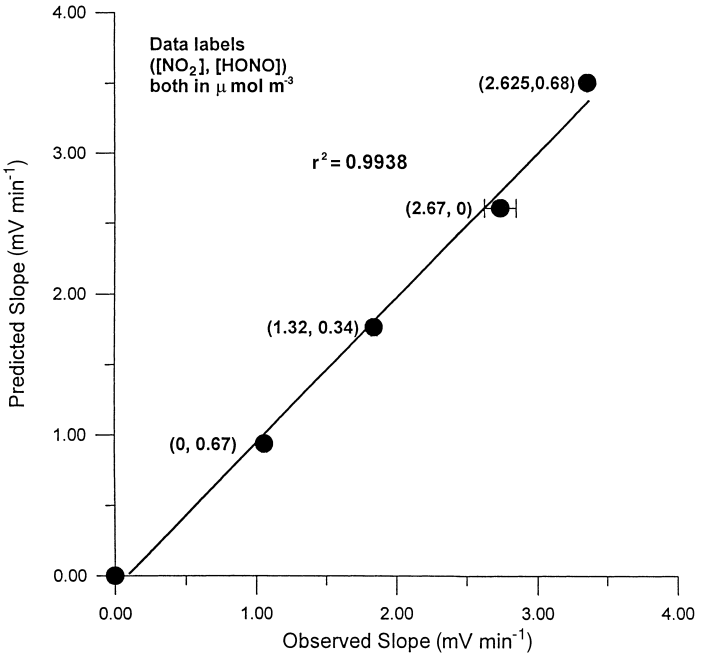

Fig. 3. Observed experimental slopes vs. those predicted from Eq. (2) for mixtures of HONO and NO_2.

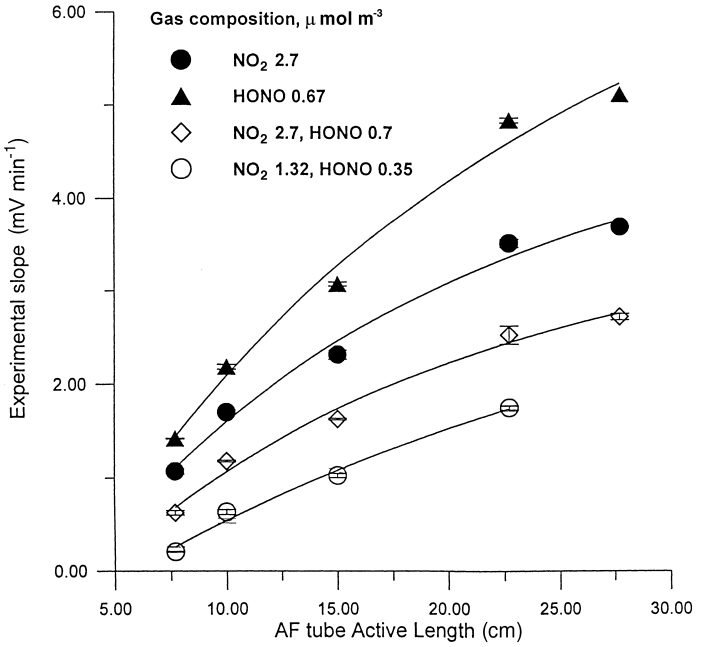

Fig. 4. Experimental slopes of AF tubes of four different active lengths for four different gas compositions.

3.3. Dependence of device response on length

The collection efficiency (f) of a diffusion based collector of the same geometry as the AF device used in the present work follows the general diffusion based collection equation below [52]

$$f = 1 - a\exp\left(\frac{-bDL}{Q}\right) \quad (3)$$

where a and b are constants, D the diffusion coefficient of the gas, L denotes the length of the tube and Q represents the volumetric sampling rate. Such an equation is applicable unless overall collection efficiencies are very low. The following are also considered. The amount of analyte collected is proportional to fQ and it is collected in a total volume of liquid within the tube that is equal to AL where A is the area of cross-section of the tube. For tubes of the same diameter, the analyte concentration C is proportional to fQ/L. Since the observed absorbance is proportional to the product of the optical path length and the analyte concentration, the observed slope is proportional only to f at a constant sampling rate. Eq. (3) can thus be written as

$$\text{Observed slope} = A_1 - A_2\exp(A_3 L) \quad (4)$$

where A_i are constants.

Type A devices of the five different lengths ranging from 77 to 277 mm were exposed to different concentrations of HONO and NO_2 in 48 separate experimental runs, all using a sampling rate of 115 ml min^{-1}. The results are presented in Table 1. As a first approximation, four different composition regimens were used, the data for each of these are shown plotted in Fig. 5, with the lines for each case indicating the best fit to Eq. (4). Within the limits of the data, the general model of Eq. (4) will appear to be appropriate.

The entire data set of Table 1 is now subjected to a two-term model in which the contributions of NO_2 and HONO are considered additive. Further, for each of these species the term within the parentheses connotes basically the collection efficiency, thus

$$\begin{aligned}\text{Slope} = {} & (1 - a_{NO_2}\exp(-b_{NO_2}L))S_{NO_2}[NO_2] \\ & +(1 - a_{HONO}\exp(-b_{HONO}L))S_{HONO} \\ & \times[HONO] \end{aligned} \quad (5)$$

Where S_{NO_2} and S_{HONO}, respectively, connotes the intrinsic reaction sensitivity of the method for NO_2 and HONO. The a- and b-terms are both affected by the specific uptake coefficient of the analyte gas by the AF tube surface. In addition, the a-term is affected by the specific geometry of the device (i.e. jacket tube i.d.; this was held constant in all present experiments) and the b-term is affected by the diffusion coefficient of the analyte gas and the sampling rate (see Eq. (4)); the sampling rate is held constant in the present experiments. Note that the collection efficiency as well as the observed analytical slope (signal) increases with decreasing value of the a-term and increasing value of the b-term. The best fit values obtained were $a_{NO_2} = 1.15$, $a_{HONO} = 1.85$; $b_{NO_2} = 0.05$, $b_{HONO} = 0.099$; and $S_{NO_2} = 1.94$, $S_{HONO} = 2.76$. Note that the ratio of the intrinsic reaction sensitivity (S_{NO_2}/S_{HONO}) is 0.70, very close to the value of 0.72 recommended for use in the manual methods.

The overall fits of the predicted slope values versus the actual observed values are shown in Fig. 5. Note that the values of the a- and b-terms indicate that the diffusive transfer of HONO to the AF tube surface is likely faster than that of NO_2. However, once the analyte is actually at the AF tube surface, the uptake probability is greater for NO_2 than for HONO. The consequence of this is that at very short tube lengths, where the depletion of the analyte in the AF surface boundary layer is less important because the analyte is plentiful, the collection efficiency for NO_2 (f_{NO_2}) is likely to be relatively higher than f_{HONO} than with longer collection tubes. The predicted collection efficiencies for NO_2 and HONO are thus shown in Fig. 6. These agree very closely with the collection efficiencies determined as described in Section 2.2.1.

It is possible to determine NO_2 and HONO separately in a mixture if results are simultaneously obtained from at least two different collection tube lengths (Eq. (5) contains two unknowns in the form of the two analyte concentrations). Greater accuracy is likely to result by using an array of collection tubes of different lengths and simple routines based on minimization of least squares [53]. Experimentally, it is easy to use individual LEDs as independent sources for each member of the array, the LEDs are inexpensive. These can be turned on one at a time and the exit optical fibers from each of the array elements can go to the same detector and be served by the same electronics. As a result, the cost of operating an array is not likely to be very much greater

Table 1
Experimental data for different device lengths and gas composition

Active length of AF device (cm)	NO_2 concentration ($\mu mol\,m^{-1}$)	HONO concentration ($\mu mol\,m^{-1}$)	Experimental slope ($mV\,min^{-1}$)	Best fit slope ($mV\,min^{-1}$)
7.7	2.65	0.00	1.09	1.12
7.7	2.65	0.00	1.05	1.12
7.7	0.00	0.67	0.20	0.25
7.7	0.00	0.67	0.21	0.25
7.7	2.63	0.67	1.41	1.35
7.7	2.66	0.68	1.43	1.37
7.7	1.32	0.34	0.64	0.68
7.7	1.32	0.34	0.61	0.68
10	2.69	0.00	1.68	1.58
10	2.70	0.00	1.72	1.59
10	0.00	0.65	0.62	0.56
10	0.00	0.68	0.65	0.58
10	2.64	0.70	2.17	2.14
10	2.63	0.68	2.20	2.13
10	1.32	0.34	1.18	1.07
10	1.33	0.34	1.17	1.07
15	2.71	0.00	2.35	2.41
15	2.72	0.00	2.28	2.42
15	0.00	0.68	1.01	1.09
15	0.00	0.69	1.04	1.10
15	2.64	0.69	3.13	3.44
15	2.64	0.69	3.01	3.44
15	1.33	0.34	1.63	1.73
15	1.33	0.35	1.62	1.74
22.7	2.69	0.00	3.49	3.31
22.7	2.69	0.00	3.49	3.31
22.7	0.00	0.65	1.73	1.45
22.7	0.00	0.64	1.77	1.41
22.7	2.70	0.67	4.83	4.78
22.7	2.70	0.67	4.72	4.78
22.7	1.32	0.33	2.46	2.36
22.7	1.33	0.33	2.44	2.36
22.7	2.72	0.00	3.58	3.34
22.7	2.71	0.00	3.53	3.33
22.7	0.00	0.68	1.73	1.49
22.7	0.00	0.68	1.77	1.50
22.7	2.67	0.69	4.95	4.82
22.7	2.69	0.69	4.88	4.82
22.7	1.34	0.34	2.60	2.40
22.7	1.34	0.34	2.63	2.40
22.7	2.69	0.00	3.69	3.73
22.7	2.69	0.00	3.70	3.73
22.7	0.00	0.72	1.59	1.75
22.7	0.00	0.73	1.65	1.76
22.7	2.64	0.72	5.09	5.42
22.7	2.65	0.72	5.15	5.42
22.7	1.33	0.36	2.75	2.72
22.7	1.34	0.37	2.70	2.74

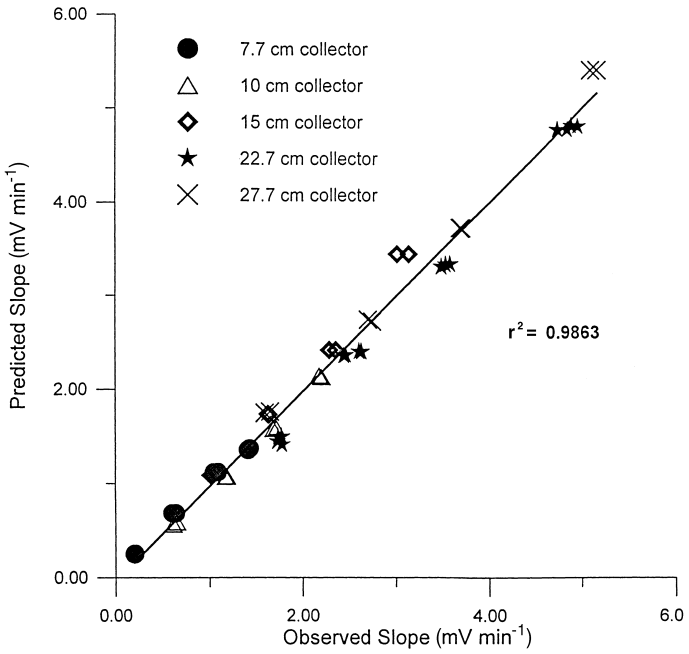

Fig. 5. Observed experimental slopes vs. those predicted from Eq. (5) for mixtures of HONO and NO_2 for five different lengths of AF collector devices.

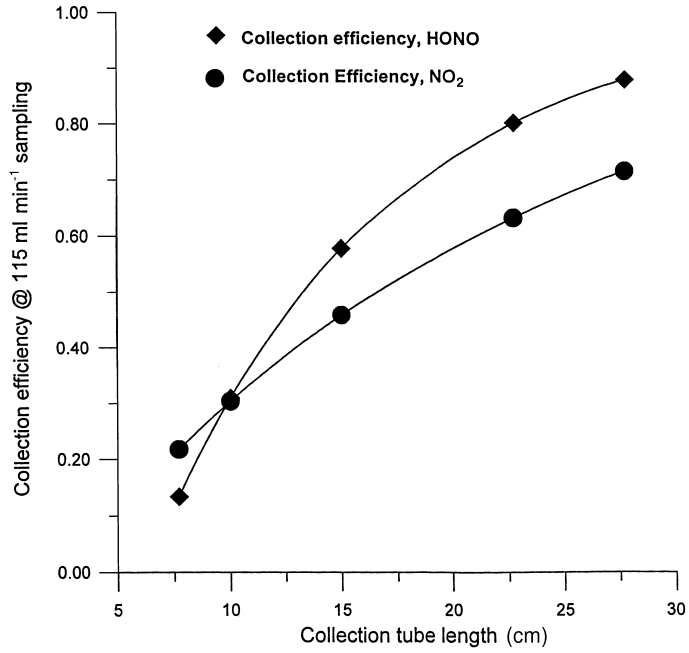

Fig. 6. Collection efficiencies for HONO and NO_2 as a function of active length of the AF device, based on Eq. (5).

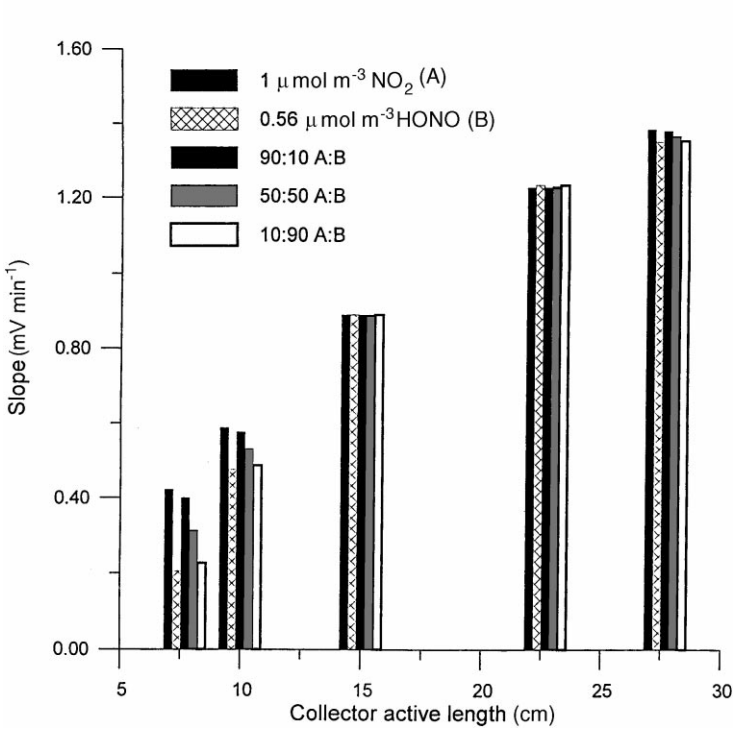

Fig. 7. Predicted slopes for five different gas compositions for five different active lengths.

than that of an individual element. Simulated results from an array of five collectors comprising of the same five collector device lengths as actually used here (not necessarily an optimum assortment for the purpose) and under the same sampling rate are shown in Fig. 7 as a bar graph, for test atmospheres containing (a) 1 μmol m^{-3} NO_2, (b) 0.56 μmol m^{-3} HONO (these concentrations were chosen such that for the intermediate 15 cm length collector, exactly the same response is observed in all cases), (c) a 90:10 mixture of a and b, (d) a 50:50 mixture of a and b, and (e) a 10:90 mixture of a and b. It would prima facie appear from Fig. 7 that although the single element response for the 15 cm collector case is exactly the same for all five compositions, the response from the entire array is different for each composition; this should enable individual determination of the two analytes.

3.4. Dependence of device response on wall thickness

Due to difficulties in the availability of material of suitable dimensions, we were able to experiment with only one other type of an AF tube where the o.d. remained the same as the type A devices but the inner diameter of the tube was ~8% smaller (and the wall 25% thicker). Note that when the internal diameter of the tube is changed without a change in the o.d. of the tube or in the jacket tube i.d. (in which it is placed), one can expect the following changes:

1. Since the internal volume of the tube is proportional to the square of the inner diameter, the concentration and hence the slope will increase inversely with the square of the diameter.
2. Mass transport will be reduced at a rate proportional to the inverse of the thickness, or a greater power thereof, depending on the nature of the transport of the analyte through the polymer.

A set of eight experiments with mixtures of NO_2 and HONO were conducted under the same conditions as in Section 3.2. The observed slopes were normalized to those of the type A devices by multiplying them with the inverse square of the ratio of the inner diameters. When processed to yield a best fit equation

in the form of Eq. (5), a good fit ($r^2 = 0.9908$) was observed with the sole difference that the best fit values of the *b*-terms were different, b_{NO_2} being 0.04 and b_{HONO} being 0.066. Note that the corresponding ratio of the *b*-terms here to those from the thinner wall type A devices are 0.78 for NO_2 and 0.67 for HONO. The wall thickness ratio is 0.8 between the two devices. Thus, the *b*-term for NO_2 decreases approximately in the ratio of the thickness, while the *b*-term for HONO decreases in proportion closer to the square of the thickness. This difference may be because the less polar NO_2 migrates through the polymer matrix itself, whereas the more polar HONO may be selectively transmitted through confined polar regions in the polymer. These results suggest that a wall thickness differentiated array of collectors may provide an even more attractive way of differentiation than a length differentiated array. We hope to report further experiments on this in the future.

In summary, we have confirmed here that not only can HONO and NO_2 be sensitively measured by simple colorimetric techniques using gas permeable liquid core waveguides but also that differentiation between these two analytes, which cannot be differentiated by the colorimetric chemistry, is possible by using more than one collector, differing in active length or wall thickness.

Acknowledgements

Much of this work was made possible by samples of various dimensions of Teflon AF tube provided by Dr. Ilia Koev of Biogeneral Inc. The help and interest of both Dr. Koev and Dr. Amos Gottlieb of Random Technologies is much appreciated. MRM's participation was made possible by a grant from the Government of Brazil which is gratefully acknowledged.

References

[1] G.P. Cobb, R.S. Braman, Chemosphere 31 (1995) 2945.
[2] G. Lammel, N. Cape, Chem. Soc. Rev. 25 (1996) 361.
[3] R.M. Harrison, J.D. Peak, G.M. Collins, J. Geophys. Res. 101 (1996) 14429.
[4] J.N. Cape, K.J. Hargreaves, R. Storeton-West, D. Fowler, R.N. Colvile, Atmos. Environ. 26A (1992) 2301.
[5] G.W. Harris, W.P.L. Carter, A.M. Winer, J.N. Pitts Jr., U. Platt, D. Perner, Environ. Sci. Technol. 16 (1982) 414.
[6] T.W. Kirchstetter, R.A. Harley, D. Littlejohn, Environ. Sci. Technol. 30 (1996) 2843.
[7] A. Febo, C. Perrino, Atmos. Environ. 29 (1995) 345.
[8] A. Sjodin, Environ. Sci. Technol. 22 (1988) 1086.
[9] J.G. Calvert, G. Yarwood, A.M. Dunker, Res. Chem. Interm. 2 (1994) 463.
[10] S. Mertes, A. Wahner, J. Phys. Chem. 99 (1995) 14000.
[11] J. Notholt, J. Hjorth, F. Raes, J. Aeros. Sci. 22 (1991) S411.
[12] M. Ammann, M. Kalberer, D.T. Jost, L. Tobler, E. Rossler, D. Piguet, H.W. Gaggeler, U. Baltensperger, Nature 395 157.
[13] M. Kalberer, M. Ammanan, F. Arens, H.W. Gaeggeler, J. Geophys. Res. 104 (1999) 13.
[14] A. Gerecke, A. Thielman, L. Gutzwiller, M.J. Rossi, Geophys. Res. Lett. 25 (1998) 2453.
[15] T.R. Rasmussen, M. Brauer, S. Kjaergaard, Am. J. Resp. Crit. Care Med. 151 (1995) 1504.
[16] T.R. Rasmussen, Ugeskrift Laeger. 156 (1994) 3907.
[17] M. Brauer, P. Koutrakis, K.D. Spengler, Environ. Sci. Technol. 23 (1989) 1408.
[18] C.W. Spicer, D.V. Kenny, G.F. Ward, I.H. Billick, J. Air Waste Manageme. Assoc. 43 (1993) 1479.
[19] B.P. Leaderer, L. Naeher, T. Jankun, K. Balenger, T.R. Holford, C. Toth, J. Sullivan, J.M. Wolfson, P. Koutrakis, Environ. Health Persp. 107 (Suppl.) (1999) 223.
[20] Z. Vecera, P.K. Dasgupta, Environ. Sci. Technol. 25 (1991) 255.
[21] D. Perner, U. Platt, Geophys. Res. Lett. 6 (1979) 917.
[22] C. Kessler, U. Platt, in: Proceedings of the 3rd European Symposium on Physico-Chemical Behavior of Atmospheric Pollution, 1984, p. 412.
[23] J.N. Pitts Jr., H.W. Biermann, R. Atkinson, A.M. Winer, Geophys. Res. Lett. 11 (1984) 412.
[24] M.D. Andres-Hernandez, J. Notholt, J. Hjorth, O. Schrems, Atmos. Environ. 30 (1996) 175.
[25] A. Febo, C. Perrino, I. Allegrini, Atmos. Environ. 30 (1996) 3599.
[26] M.O. Rodgers, D.D. Davis, Environ. Sci. Technol. 23 (1989) 1106.
[27] W.L. McClenny, U.S. E.P.A., Atmospheric Research and Expos. Assess. Laboratory, Research Triangle Park, NC, personal communication, 2000.
[28] M. Ferm, A. Sjodin, Atmos. Environ. 19 (1985) 979.
[29] I. Allegrini, F. De Santis, V. Di Palo, A. Febo, C. Perrino, M. Possanzini, Sci. Total Environ. 67 (1987) 1.
[30] M. Brauer, P. Koutrakis, J.D. Spengler, Environ. Sci. Technol. 23 (1989) 1408.
[31] A. Sjodin, M. Ferm, Atmos. Environ. 19 (1985) 985.
[32] A. Sjodin, Environ. Sci. Technol. 22 (1988) 1086.
[33] B.R. Appel, A.M. Winer, Y. Tokiwa, H.W. Biermann, Atmos. Environ. 24A (1990) 611.
[34] A. Febo, C. Perrino, M. Cortiello, Atmos. Environ. 27A (1993) 1721.
[35] S.A. Penkett, F.J. Sandalls, B.M.R. Jones, VDI-Ber. 270 (1977) 47.
[36] J.E. SicklesII II, L.L. Hodson, Atmos. Environ. 23 (1989) 2321.
[37] A.S. Geyh, J.M. Wolfson, P. Koutrakis, J.D. Mulik, E.L. Avol, Environ. Sci. Technol. 30 (1997) 2326.

[38] P.K. Simon, P.K. Dasgupta, Z. Vecera, Anal. Chem. 63 (1991) 1237.
[39] Z. Vecera, P.K. Dasgupta, Anal. Chem. 63 (1991) 2210.
[40] P.K. Simon, P.K. Dasgupta, Anal. Chem. 65 (1993) 1134.
[41] J. Slanina, G.P. Wyers, Z. Fres, Anal. Chem. 350 (1994) 467.
[42] B.E. Salzman, Anal. Chem. 26 (1954) 1949.
[43] J.P. Lodge Jr. (Ed.), Methods for Air Sampling and Analysis, 3rd Edition, Lewis, Ann Arbor, MI, 1989, p. 389.
[44] P. Dress, H. Franke, Appl. Phys. B 63 (1996) 12.
[45] P. Dress, H. Franke, Rev. Sci. Instrum. 68 (1997) 2167.
[46] W. Yao, R.H. Byrne, R.D. Waterbury, Environ. Sci. Technol. 32 (1988) 2646.
[47] P.K. Dasgupta, Z. Genfa, S.K. Poruthoor, S. Caldwell, S. Dong, Anal. Chem. 70 (1998) 4661.
[48] P.K. Dasgupta, H.S. Bellamy, H. Liu, J.L. Lopez, E.L. Loree, K. Morris, K. Petersen, K.A. Mir, Talanta 40 (1993) 53.
[49] Z. Vecera, P.K. Dasgupta, Environ. Sci. Technol. 25 (1991) 255.
[50] P.K. Dasgupta, S. Dong, H. Hwang, H.C. Yang, Z. Genfa, Atmos. Environ. 22 (1988) 949.
[51] C. Huygen, R.W. Lanting, Atmos. Environ. 9 (1975) 1027.
[52] P.K. Dasgupta, ACS Adv. Chem. Ser. 232 (1993) 41.
[53] S. Walsh, D. Diamond, Talanta 41 (1994) 561.